A Review of the Dimensionless Parameter Scaling Studies

by J.G. Cordey, B. Balet, D. Campbell, C.D. Challis, J.P. Christiansen,
C. Gormezano, C. Gowers, D. Muir, E. Righi, G.R. Saibene, P.M. Stubberfield
and K. Thomsen

JET Joint Undertaking, Abingdon, OXON, OX14 3EA U.K.

ABSTRACT

The theoretical basis of the dimensionless parameter scaling technique is derived and the limitations in its application are discussed. The use of the technique is illustrated by the production on JET of steady state ITER similarity pulse having the same β and collisionality as the ignited ITER. The key issue of the scaling of the transport with the main dimensionless parameter ρ^* is discussed in detail. Finally possible shortcomings of the technique are examined.

I. INTRODUCTION

One of the most difficult problems facing the designers of the next generation of fusion experiments is to estimate accurately the energy confinement and fusion performance of a particular design. As yet there is no fully tested 1-D model of the energy particle transport in a tokamak and so one presently has to resort to 0-D global energy confinement projections. Since these don't give the plasma profiles this approach is rather restricted.

An alternative approach which is discussed in this paper is the similarity approach or as it sometimes known the "windtunnel" approach. The basic idea is to design discharges with as many dimensionless parameters as possible at the values that they will have in the next generation of experiments. This can be achieved for all of the dimensionless parameters thought to have an influence on the transport, except the dimensionless Larmor radius parameter $\rho^*(\equiv \rho_i/a)$, where ρ_i is the Larmor radius and a the machine minor radius. Once the dependence of the transport on ρ^* has been determined both by experiments on a single machine and on machines of different sizes, then one can scale the transport coefficient, and as we shall show, the temperature profiles in a simple manner to establish the conditions in a new machine.

The key feature of this similarity approach is that details of the dependence of the transport on quantities such as the safety factor profile q, or the dimensionless profile factor $\eta(\equiv$ DlogT/Dlogn) need not be determined.

The structure of the paper is as follows, in Section II, the theoretical basis behind the technique is presented, then in Section III the JET ITER similarity pulses are described, in Section IV the ρ^* scaling of ELMy H-modes on JET is presented from both a global and local point of view, then in Section V the reasons for completing dimensionless identity experiments are discussed. In Section VI the shortcomings of the technique are examined, and finally in Section VII we examine the connection between global scaling expressions and the ITER similarity pulses.

II. THEORETICAL BASIS OF THE TECHNIQUE

It has been shown by Kadomtsev [1] and Connor and Taylor [2] that the expression for the thermal diffusivity can be expressed in the form

$$\chi = \frac{T}{B} \quad F\,(\rho^*, \beta, \nu^*, q, a/R, \eta, \kappa, \ldots) \qquad (1)$$

provided the turbulence has a scale length larger than the Debye length and the turbulence is not driven by atomic processes.

The smallest of the dimensionless parameters is ρ^* so we can expand in ρ^* without any loss of generality

$$\chi = \frac{T}{B} \quad [\rho^{*-1}\, H\,(\beta, \nu^*, \ldots) + I\,(\beta, \nu. \ldots) + \rho^*\, G(\beta, \nu^*, \ldots)] \qquad (2)$$

The first term in the square brackets describes the loss process arising from free flow along stochastic field lines with a correlation length of order of the minor radius a, the second term is the Bohm term where the turbulence correlation width is of order $\sqrt{\rho_i a}$ and finally the third term is the gyro-Bohm term where the turbulence correlation width is a Larmor radius ρ_i. Most theories of plasma transport are of the gyro-Bohm form, although there are some theories which give rise to Bohm diffusivity. Short MHD events such as sawteeth or ELMs can give rise to stochastic energy loss. Measurements of plasma turbulence in Tokamaks have usually found the correlation width to be of the order of the ion gyro radius supporting the gyro-Bohm theories.

If one of the three terms of equation (2) is dominant across the profile then in principle we do not need to determine its dependence on β, ν^* etc, the value of the function across the profile is sufficient.

In order to keep the dimensionless parameters $\beta(\equiv nT/B^2)$, $\nu^*(\equiv na/T^2)$ and q fixed then the plasma density n, temperature T and current I should scale as follows:

$$n \propto B^{4/3} a^{-1/3}$$

$$T \propto B^{2/3} a^{+1/3} \qquad (3)$$

$$I \propto Ba$$

$$W \propto B^2 a^3$$

The power and the gas input rate are adjusted to reproduce the above scalings. From Eq. (2) together with ρ^* ($\equiv T^{1/2}/Ba$) $\propto B^{-2/3} a^{-5/6}$ the scaling of the thermal diffusivity and the energy confinement time may be derived for discharges satisfying the relations of Eq. (3). For the three different types of transport considered in Eq. (2) we get:

gyro-Bohm	$\chi \propto a^2 B\rho^{*3}$,	$\tau_\varepsilon \propto \rho^{*-3}/B \propto a^{5/2} B$	
Bohm	$\chi \propto a^2 B\rho^{*2}$,	$\tau_\varepsilon \propto \rho^{*-2}/B \propto a^{5/3} B^{1/3}$	(4)
Stochastic	$\chi \propto a^2 B\rho^{*}$,	$\tau_\varepsilon \propto \rho^{*-1}/B \propto a^{5/6} B^{-1/3}$	

Thus the scaling of τ_ε with B is very different for the different types of transport.

III. ITER SIMILARITY PULSES

During the 1995 JET experimental campaign several ITER similarity discharges were set up. With the power that was available (20 MW) it was only possible to reach the β's of the ITER operating point (β_n ($\equiv \beta aB/I$) = 2.3) at fields up to 2T. An example of the time evolution at a steady state ELMy H-mode discharge with the ITER β_n and collisionality is shown in Fig. (1a), and the density and temperature profiles are shown in Fig. (1b). The left hand ordinate in all of the graphs is the JET value of the parameter and the right hand ordinates show the scaled ITER values obtained from Eq's (3) and (4). For the power a gyro-Bohm scaling has been assumed in the graph giving about 80 MW. With the projected α power of 300 MW minus Bremsstrahlung of 110 MW ignition would be easily achieved. If a Bohm scaling is assumed then the required power would be over 600 MW, and only driven operation would be possible with Q around 4. Thus we see that it becomes crucial to determine the scaling of the transport with ρ^*.

IV. THE P* SCALING OF ELMY H-MODES

The first experiments on the ρ^* scaling of ELMy were completed on DIII-D [3], where the confinement both globally and locally was found to have a gyro-Bohm scaling. Similar experiments on JET at 1MA/1T and 2MA/2T also showed a gyro-Bohm scaling [4]. The pulse

characteristics for the two pulses are reproduced in Figs. 2a) and b) and a summary of the global confinement characteristics is given in Table 1. From the table one can see that the density and stored energy are in the correct ratio so the two pulses form a similarity pair according to equation (3). The confinement scales as the toroidal field B indicating a gyro-Bohm confinement.

Table I

Pulse no.	B(T)	1 (MA)	$\langle n_e \rangle / 10^{19}$ M-3	P(MW)	Wth(MJ)	τ_{th}
35171 (25.8s)	1	1	2.2	5.03	0.85	0.17
35156 (16.1s)	2	2	5.5	9.47	3.2	0.35

A full local transport has been completed for both these pulses using the TRANSP code. The ratio of the χ's of the 2T and 1T pulses are shown in Fig. (3) normalised to the Bohm scaling. The χ_{eff}'s have been calculated in the same manner as Perkins et al [5].

$$\chi_{eff} = q/(n_e T_e - n_i T_i)/a$$

where q is the total conducted heat flux. This Figure shows that the transport is gyro-Bohm across the profile.

V. DIMENSIONLESS IDENTITY EXPERIMENTS

To confirm that the dimensionless parameter technique is valid and that there are no other important parameters involved in the confinement then ρ^*, β, ν^*, q etc, a series of dimensionless identity experiments have been carried out between JET and DIII-D. In these experiments one attempts to keep all of the dimensionless parameters fixed, including ρ^*. These are really truly analogous to windtunnel experiments in that the engineering parameters are different between the two experiments, and all the dimensionless physics parameters are the same. From equation (4) it can be seen that whatever form the transport takes the τ_ε should be inversely proportional to B. Other times such as the time between ELMs should also vary as 1/B, if a good profile match has been obtained in the edge region.

The preliminary results which are presented in reference (6) do indeed show that the energy confinement accurately scales as predicted, there is however a larger discrepancy in the scaling of the ELM frequency between the two machines.

VI. POSSIBLE SHORTCOMINGS OF THE TECHNIQUE

There are two possible shortcomings of the similarity approach. The first is if the dominant transport process were to change with ρ^*, i.e. with machine size; an example of this is confinement near the L-H threshold. The second is that the effects of profile mismatches on predictions are not easy to estimate. An example of how a small profile mismatch in the edge region has a dramatic effect on the confinement is given at the end of this section.

(a) Confinement in the vicinity of the H-mode threshold

A pair of similarity discharges at higher toroidal fields (1.7T and 3T) than the pair presented in Table I were obtained during the 1995 campaign. The main parameters for these pulses are listed in Table II, from the ratio of confinement times of the two pulses it can be seen that there is no dependence on toroidal field, thus from Eq. (4) the scaling of the confinement is much worse than gyro-Bohm being between Bohm and Stochastic.

Table II

Pulse no.	B(T)	1 (MA)	$\langle n_e \rangle / 10^{19}$ M-3	P(MW)	Wth	τth
33140 (16.6s)	1.7	1.6	3.6	6.6	2.3	0.35
33131 (15.6s)	3	2.8	7.6	21	7.3	0.35

Examination of the local transport for these two pulses Fig. (4) shows that the degradation in the transport of the high field pulse relative to the lower field pulse is in the edge region. The excess power loss is thought to be due to the ELMs.

A rough calculation of the power lost by the ELMs in the high field pulse is approximately 1/3 of the input power. In the absence of this loss, the energy confinement would revert to gyro-Bohm.

The reason that the ELM loss is relatively more significant in the high field pulse is thought to be due to the fact that the power level in this pulse is quite close to that of the L-H threshold, and after each ELM the pulse goes back to L-mode. This conjecture however needs to be confirmed by further experiments.

(b) Sensitivity of confinement to the edge profile

During the ρ^* scaling experiments the same stored energy was obtained in two discharges with different gas fuelling rates; medium and high. However to achieve the same stored energy the power had to be increased from 9 MW in the medium fuelled discharge to 12.5 MW in the high

gas fuelled discharge, reducing the confinement time by some 40%. Indeed if one further increases the fuelling rate one can reduce the energy confinement even further and push the discharge back into the L-mode state [7].

The time development of the two pulses is shown in Fig. 5. The basic global parameters, such as the stored energy and density are essentially identical, however the ELM frequency is some 4 times higher in the strongly fuelled pulse. A close inspection of the profiles in the edge region, see Fig. 6, reveals a slightly broader density profile in the high gas fuelled pulse.

Thus we see that relative small changes in the profile in the edge region strongly affect the nature of the ELMs and also the global energy confinement time. These two effects may not be directly connected in that it is not clear that the energy loss by the ELMs accounts for the change in confinement in this case. However the key point here is that to produce perfectly matched similarity pulses one should also endeavour to scale all particle source rates in the appropriate manner.

VII. COMPARISON WITH GLOBAL SCALING EXPRESSIONS

It is interesting to compare the energy confinement in these ITER similarity pulses and ρ^* scans with the existing global scaling expressions which are being used to predict the performance of ITER. The dimensionally correct form of the ITERH93P scaling, which satisfies the gyro-Bohm constraint, expressed in engineering variables has the form,

$$\tau_{\varepsilon th}^{ITERH93P'} = 0.031\, I^{1.05}\, B^{0.36}\, n_e^{0.21}\, A^{0.38}\, R^{1.86}\, \varepsilon^{-0.14}\, \kappa^{0.65}\, P^{-0.69} \qquad (5)$$

This is very close to the precise ITERH93-P scaling which is

$$\tau_{\varepsilon th}^{ITERH93P} = 0.036\, I^{1.06}\, B^{0.32}\, n^{0.17}\, A^{0.41}\, R^{1.79}\, \varepsilon^{-0.11}\, \kappa^{0.66}\, P^{-0.67} \qquad (6)$$

In Fig. (7) the dimensionless confinement time $B\tau_\varepsilon$ is shown versus the product of B and the scaling expression of eq. (5). All the data except the high gas fuelled are within 13% of the scaling expression. The high gas fuelled pulse is some 40% below the scaling expression. Mixing this type of pulse with lower gas fuelled pulses may be one of the reasons for the large data scatter in the ITER ELMy data base. Thus it is important that the pulses in the data base are characterised with respect to this parameter.

ACKNOWLEDGEMENTS

The authors gratefully acknowledge many useful discussions with T.C. Luce and C.C. Petty of General Atomics.

REFERENCES

(1) B.B. Kadomtsev, Sov. J. Plasma Phys. 1 295 (1975).
(2) J.W. Connor and J.B. Taylor, Nucl. Fusion 17, 1047 (1977).
(3) C.C. Petty, T.C. Luce, K.H. Burrell et al. Physics of Plasmas Vol. 2, 2342 (1995).
(4) B. Balet, et al. Proceedings EPS Conference Bournemouth (1995).
(5) F.W. Perkins, et al. Phys. Fluids B **5** (1993) 477.
(6) C.C. Petty, et al. EPS Kiev 1996.
(7) G. Saibene, et al. PSI Conference 1996.

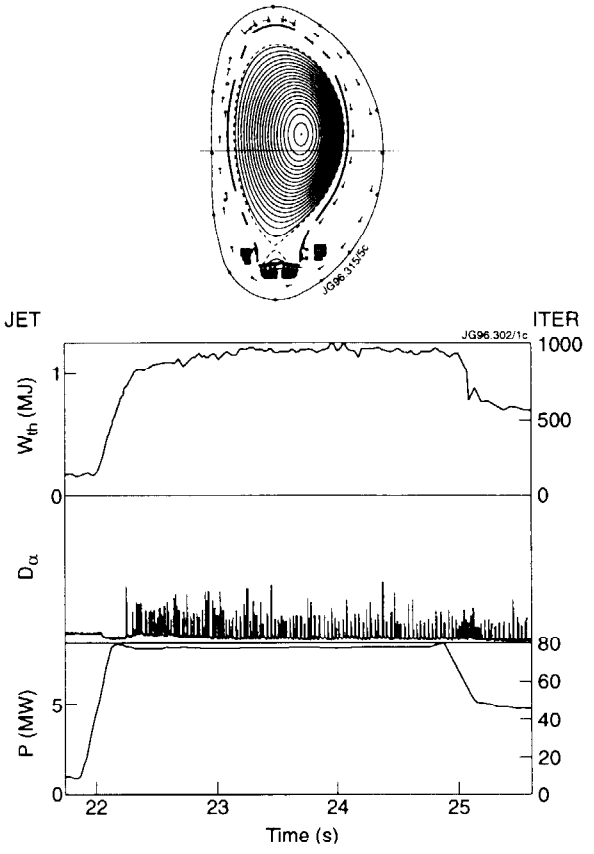

Fig. 1 (a) Thermal stored energy, D_α trace and total input power versus time. The left hand axis is the JET pulse 35174 (β_{nth} = 2.3, $q_\psi 95$ = 3.2), the right hand axis are the scaled ITER values.

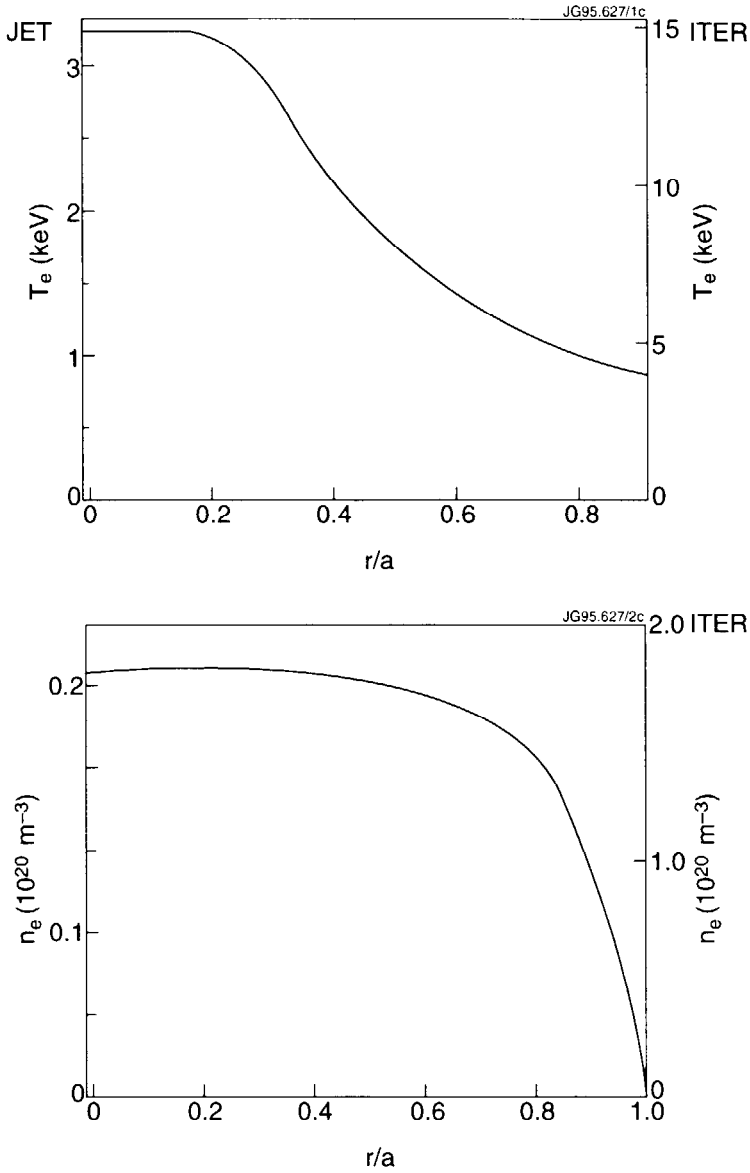

Fig. 1 (b) The temperature and density profiles of pulse 35174, the left hand axis are the JET values, the right hand axis are the scaled ITER values.

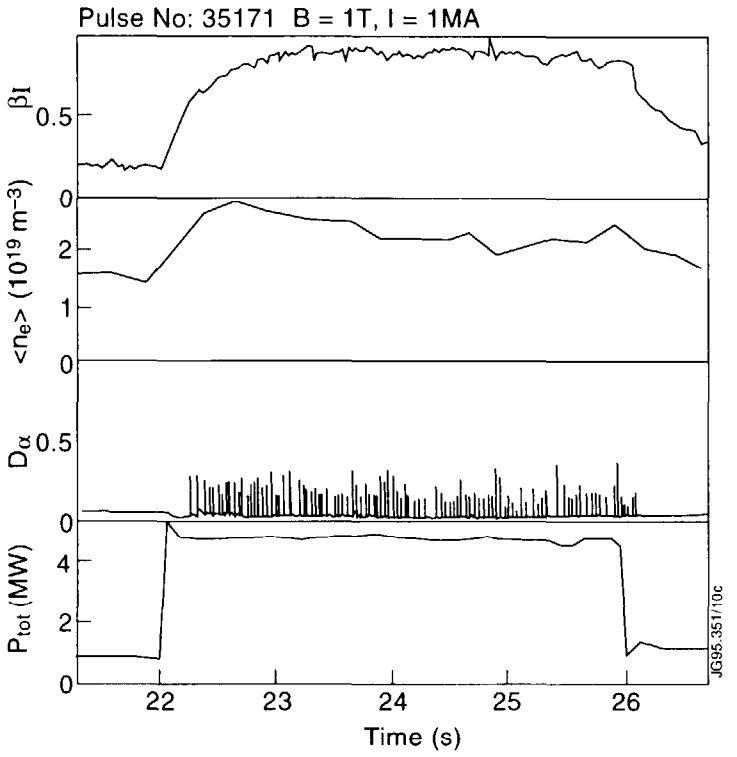

Fig. 2 (a) Time development of the 1MA/1T pulse 35171, β_n, volume average density, D_α and total input power.

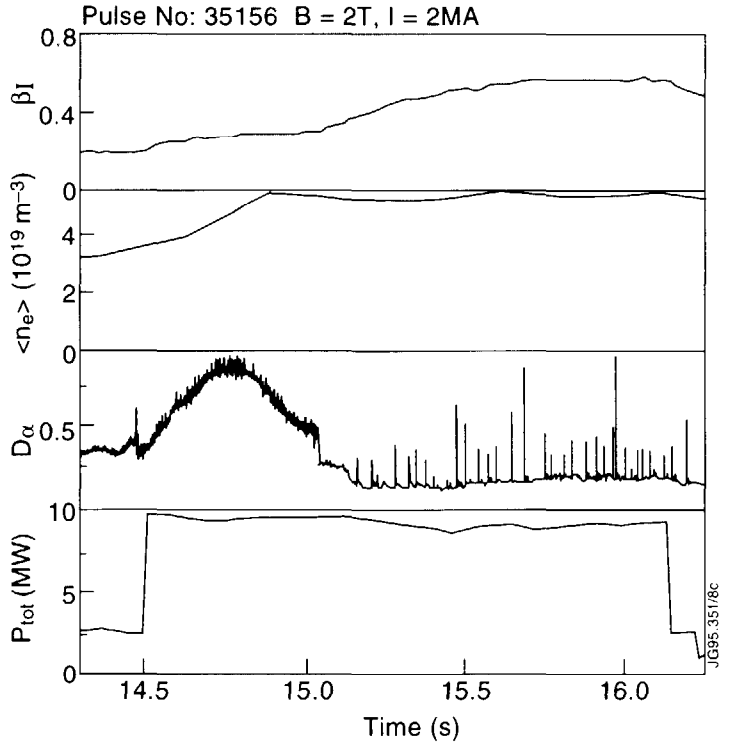

Fig. 2 (b) Time development of the 2MA/2T pulse 35156, β_n, volume average density, D_α and total input power.

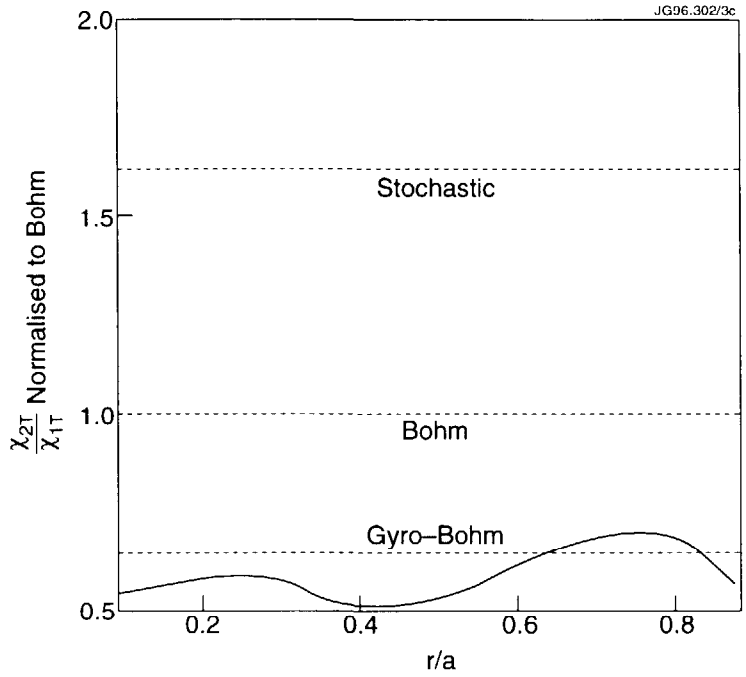

Fig. 3. Ratio of the χ_{eff}'s of the 2T pulse (35156) to the 1T pulse (35171) normalised to Bohm versus the normalised radius r/a.

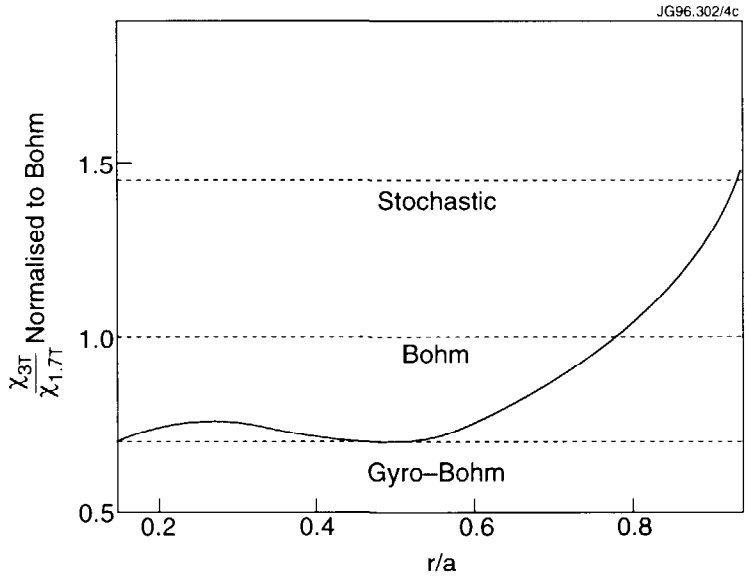

Fig. 4. Ratio of the χ_{eff}'s of the 3T pulse (33131) to the 1.7T pulse (33140) normalised to Bohm versus the normalised radius r/a.

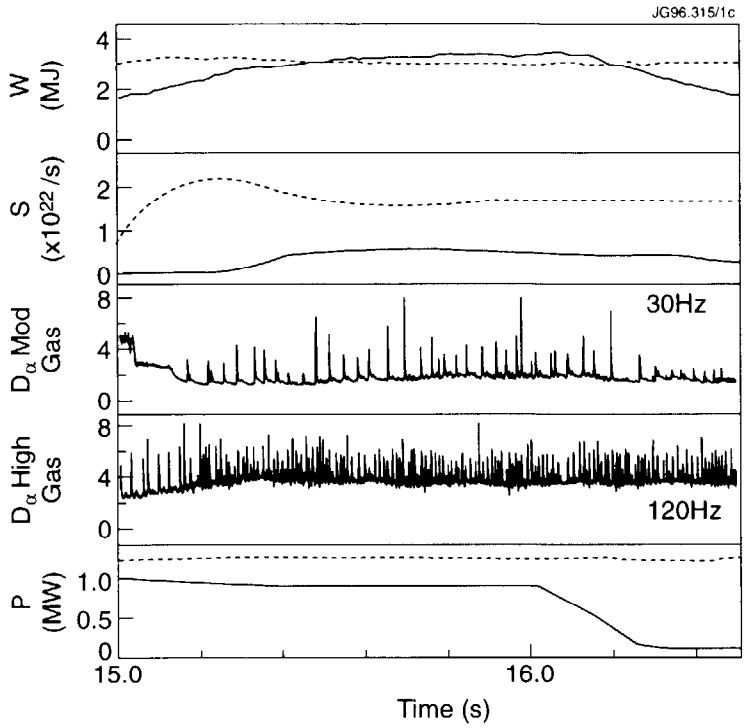

Fig. 5. Stored energy, gas fuelling rate, $D\alpha$ for low fuelling pulse (35156), $D\alpha$ for high fuelling pulse (35176), total input power versus time. The dotted curve is the high gas fuelled pulse (35176), the continuous line is for the low fuelled pulse (35156).

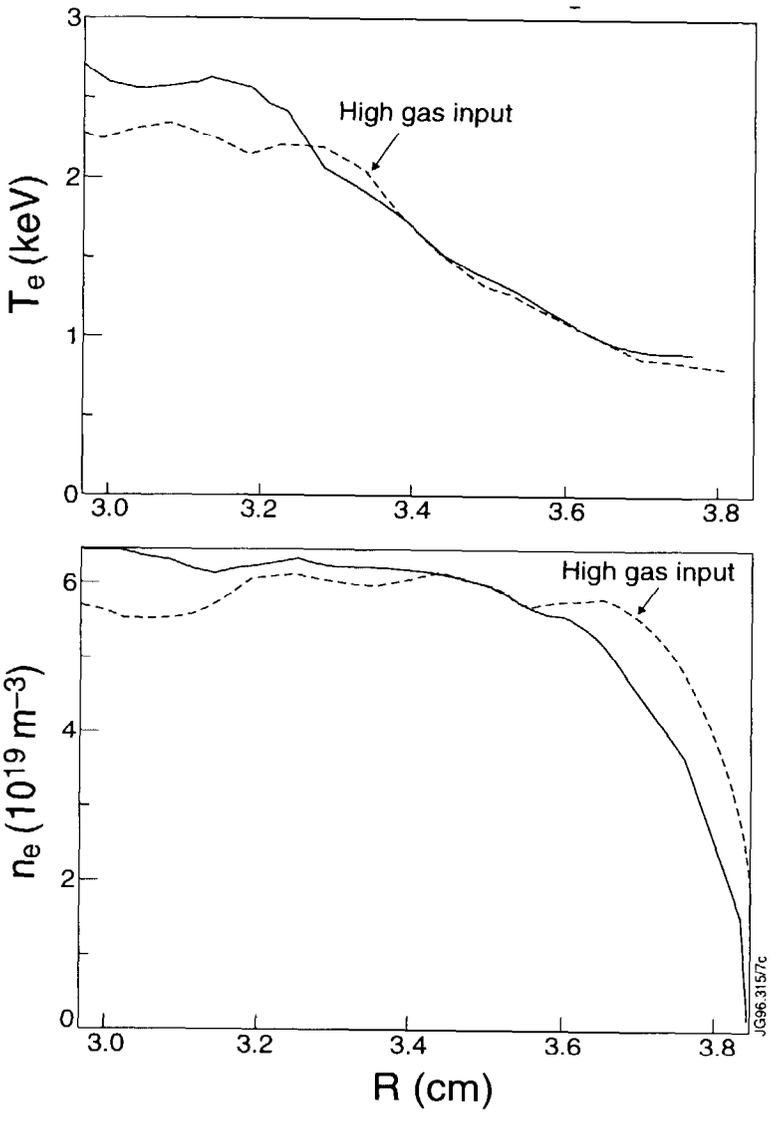

Fig. 6. Temperature and density profiles for the two pulses (35156, 35176) versus normalised radius.

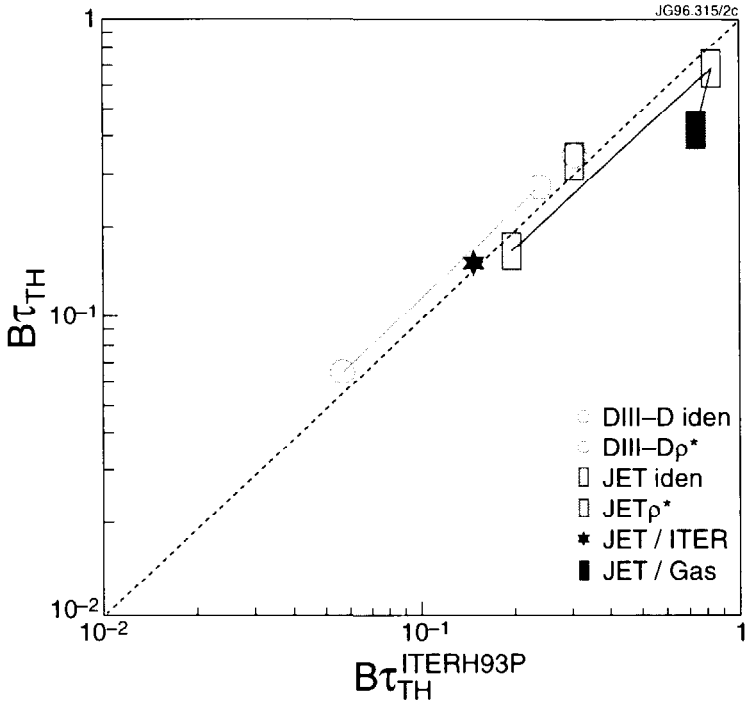

Fig. 7. The dimensionless thermal confinement time versus the product of the scaling expression of equation (5) and the toroidal field. The JET points are the ρ scan described in Section IV, the ITER similarity pulse is from Section III, the high gas input pulse is from Section V, the DIII-D ρ* scan was from Reference III, and the JET /DIII-D identity pulse is from T. Luce (private communication).*